Simplified flame models and prediction of the thermal radiation emitted by a flame front in an outdoor fire

Jean Louis Rossi, Khaled Chetehouna, Anthony Collin, Basiliu Moretti, Jean Henri Balbi

Simplified flame models and prediction of the thermal radiation emitted by a flame front in an outdoor fire

JEAN-LOUIS ROSSI[A], KHALED CHETEHOUNA[B,*], ANTHONY COLLIN[C], BASILIU MORETTI[A] AND JACQUES-HENRI BALBI[A]

[A] Université de Corse, Systèmes Physiques pour l'Environnement

U.M.R.-C.N.R.S. 6134

Campus Grossetti, BP 52 20250 Corte, France

Phone: (+33) 495 450 161; Fax: (+33) 495 450 162

[B] ENSI de Bourges, Institut PRISME UPRES EA 4229 EP-RES, 88 Boulevard Lahitolle, 18020 Bourges Cedex, France

Phone: (+33) 248 484 065; Fax: (+33) 248 484 050

[C] Laboratoire d'Energétique et de Mécanique Théorique et Appliquée

U.M.R.-C.N.R.S. 7563

02 Avenue de la forêt de Haye, BP 160, 54504 Vandoeuvre cedex, France

Phone: (+33) 383 595 604; Fax: (+33) 383 595 551

[*] **Corresponding Author**. Email: khaled.chetehouna@ensi-bourges.fr

Abstract –

This paper proposes a comparison between two simplified flame models. The first flame model uses the radiant surface approach with a new analytical expression for the heat flux. The second one is derived from the Radiative Transfer Equation. The fire front has been considered as a line characterized by some geometric and physical parameters. Two assumptions are used to model the flame either a radiant plane or a volumetric flame. The flame parameters have been identified from experiments using video records and applying an inverse method. These two models were tested against fires carried out in a fire tunnel and found to perform very well considering the complicate nature of the flame geometry and flame characteristics. The need to determine the heat flux from a large scale fire has lead to make a number of assumptions. By means of the proposed modeling, this study tries to determine the extent to which the range of assumptions made disqualifies some simplified flame models from use.

Keywords: Flame models, heat flux, fire experiments, large scale fires.

INTRODUCTION

Every year outdoor fires are responsible for loss of human life and environment damages. Radiant heat transfer is the main mechanism of heat transfer for wildland fires. The other two being convection and conduction but thermal radiation is commonly acknowledged as the dominant mode of heat transfer for large scale fires. So, the need to determine the radiant heat flux has lead to the development of number of flame models (Viskanta, 2008; Sacadura, 2005). Furthermore, accurate information about radiant heat flux is important in a number of applications. These include: establishing safety distances for firefighters (Zàrate *et al.*, 2008; Raj, 2008) and developing models of fire spread (Morvan *et al.*, 2008; Séro-Guillaume *et al.*, 2008; Balbi *et al.* 2007). Due to the complexity of fire mechanisms, modeling of the flame structure has been carried out with different degrees of simplification from empirical models to software packages implementing computational fluid dynamics of reacting flows.

The purpose of this paper is to compare two simplified radiative flame models. The first flame model uses the radiant surface approach and the second treats the flame front as a volumetric source. Radiative emission from the whole flame is then determined from the geometry of the flame and the properties of the fire front. In addition, this work tries using these two simplified radiative flame models to determine the extent to which the range of assumptions made disqualifies some radiative modeling from use.

FLAME MODELS AND PREDICTION OF THERMAL RADIATION

In forest fires research literature, it is generally admitted that the radiation from flames is the dominant mechanism of fuel bed preheating (Viegas, 2004). The flame is commonly modeled as a radiant surface with a given height, constant temperature and

emissivity. The radiant surface hypothesis has previously been used by several authors as a beginning to establish, in varying ways, simplified radiative flame models to be used in linear fire front model (Zàrate *et al.*, 2008; Balbi *et al.* 2007; Chetehouna *et al.* 2005; Knight and Sullivan, 2004, Morandini *et al.*, 2001; Dupuy, 2000). In this section, two simplified radiative flame models are presented in order to compare the theoretical radiative heat fluxes with the experimental ones measured by a wireless thermal sensor. The first flame model (model I) uses the radiant surface approach and the second one (model II) is derived from the Radiative Transfer Equation (Siegel and Howell, 2002).

Model I

The aim of this study is to find a new analytical expression of the heat flux emitted by a flame front of a wildland fire. It is assumed that the flame front is generalized into a simplified geometry: a finite rectangular area inclined with an angle γ. The target is considered to be a differential receptor element parallel to the flame area and located in front of its centre just above the vegetation (see fig. 1).

View factor

In radiative heat transfer, the view factor $F_{i\to j}$ is a geometrical parameter. This parameter determines the proportion of all the radiation which leaves surface *i* and strikes surface *j*.

The view factor between the point *M* (sensor) and the flame front is given as (Siegel and Howell, 2002)

$$F_{f\to M} = \frac{1}{\pi}\int_S \frac{\cos\theta_{fl}\cos\theta_M}{R^2} dS \qquad (1)$$

with S the flame surface and dS its element. R is the distance between the point M and the element dS. θ_{fl} and θ_M are respectively the angle between R and the normal of fire front and the angle between R and the normal of the target.

The unit vector normal to the flame and to the sensor are respectively denoted $\vec{N}$ and $\vec{n}$. $\vec{i}_n$ is the unit vector on the straight line (*QM)* and d_o is the distance *PM* (see Fig. 1).

So:

$$\cos\theta_M = -\vec{n}.\vec{i}_n = \frac{1}{R}(x\cos\gamma - z\sin\gamma) \qquad (2a)$$

$$\cos\theta_{fl} = \vec{N}.\vec{i}_n = \frac{x}{R} \qquad (2b)$$

$$R = \sqrt{d_o^2 + y^2} \qquad (2c)$$

If expressions (2a), (2b) and (2c) are inserted in (1) and after a first integration over y-axis, the following expression is obtained:

$$F_{f\to M} = \frac{1}{\pi}\int_{z_{\min}}^{z_{\max}} \frac{1}{d_o^3}(x^2\cos\gamma - z\,x\sin\gamma)\left(\frac{d_o\,L}{d_o^2 + L^2} + \arctan\frac{L}{d_o}\right)dz \qquad (3)$$

Now, using the relationships: $z = x\tan\psi$, $d_o = \dfrac{x}{\cos\psi}$. Hence, the view factor can be written:

$$F_{f\to M}(\mathbf{M}) = \frac{1}{\pi}\int_{\psi_{\min}}^{\psi_{\max}} \cos(\gamma+\psi)\left(\arctan\left(\frac{L\cos\psi}{x}\right) + \frac{\dfrac{L\,x}{\cos\psi}}{\left(\dfrac{x}{\cos\psi}\right)^2 + L^2}\right)d\psi \qquad (4)$$

where $\psi_{\min} = -\gamma$, $\psi_{\max} = \theta_f - \gamma$ and θ_f the angle between (O_0M) and (MF).

Finally, after a last integration and some calculations, it can be determined an analytical expression for the view factor:

$$F_{f\to M}(\mathbf{M}) = \frac{1}{2\pi}\left(\frac{2L\arctan\left(\frac{2x\sqrt{L^2+x^2}\sin\theta_f}{L^2\cos(\gamma-\theta_f)+(L^2+2x^2)\cos\theta_f} \right)\cos\gamma}{\sqrt{L^2+x^2}} - 2\arctan\left(\frac{-L\cos(\gamma-\theta_f)}{x} \right)\sin\theta_f \right) \quad (5)$$

In order to determine the angle θ_f, it is necessary to consider two situations: (a) the receptor is beneath the flame and (b) the receptor is ahead of the flame (see Fig. 2). In the first case, the following expression is found:

$$\theta_f^a = \frac{\pi}{2} \quad (6a)$$

and in the second case:

$$\theta_f^b = \arctan\left(\frac{l_f\cos\gamma}{r - l_f\sin\gamma} \right) \quad (6b)$$

where l_f is the length of the flame and *r* is the distance between the base of the fire front and the sensor at the position *M*.

Heat flux

In order to evaluate the thermal radiation reached by a sensor located at a distance *r* from the fire front (see Fig. 1), the solid flame model is proposed which considers the visible flame to be a geometrical body that emits radiative energy uniformly throughout its surface like a blackbody (Zàrate *et al.*, 2008; Knight *et al.*, 2004; Sullivan *et al.*, 2003). Consequently, it is assumed a second approximation: the non-visible zones of the flame are not taken into account. Indeed, Baukal and Gebhart (1997) reported that non-visible radiation was found to be negligible compared with the total heat flux.

Therefore, the heat flux at the position *M* can be given by the analytical expression below:

$$\Phi_I^{th}(\mathbf{M}) = \tau\,\varepsilon\,B\,T_f^4\,F_{f\to M} \qquad (7)$$

where τ is the atmospheric transmissivity, ε is the equivalent flame emissivity, *B* is the Stephan-Boltzmann constant, T_f is the flame average temperature and $F_{f\to M}$ the view factor which is given by Eq. (5).

Model II

In this mathematical modeling, the flame is supposed to have a area A_f on top of the fuel bed, a height h_f, a tilt angle γ, an average temperature T_f and an extinction coefficient K_f.

The Radiative Transfer Equation can be written (Siegel and Howell, 2002):

$$\frac{dI(s)}{ds} = -(K(s)+\sigma(s))\,I(s) + K(s)\,I_b(s) + \frac{\sigma(s)}{4\pi}\int_{\omega=0}^{4\pi} I(s,\omega_i)\,\tilde{\Phi}(\omega_i,\omega)\,d\omega_i \quad (8)$$

where *I* is the radiative intensity, *K* and σ are respectively the absorption and scattering coefficients. $\tilde{\Phi}$ is the phase function and ω_i is the solid angle. If we consider a thin flame approximation, the integration of this equation through the flame-fuel bed geometry (see Fig. 3) leads to:

$$I(s) = K_f\,\frac{BT_f^4}{\pi}\,e^{-K_v(s-s_3)}\int_{s_1}^{s_2} d\bar{s} + K_v\int_{s_1}^{s_2} I_b(\bar{s})\,e^{-K_v(s-\bar{s})}\,d\bar{s} \qquad (9)$$

where I_b is the radiative intensity of Blackbody.

The radiative heat flux received by the target (sensor) can be calculated by the integration of the radiative intensity over the solid angle. This heat flux is given by the following expression:

$$\Phi_{II}^{th}(\mathbf{M}) = K_f \frac{BT_f^4}{\pi} \int_{\Omega_f} \frac{\vec{s}.\vec{n}}{XM^2} d\Omega \qquad (10)$$

where Ω_f is the flame domain, B is the Stefan-Boltzmann constant, $\vec{s}$ and $\vec{n}$ are respectively the unit vector of the line (O_1M) and the unit normal vector of the sensor. The points X and M are respectively the positions of a flame elementary area and the target. After some calculation done by Séro-Guillaume *et al.* (2008) and Chetehouna *et al.* (2008) this relationship can be expressed as:

$$\Phi_{II}^{th}(\mathbf{M}) = K_f \frac{BT_f^4}{\pi} \int_{A_f} \frac{dx_o dy_o}{r \sin^2 \beta \cos\gamma} \times \qquad (11)$$
$$[(\sin\phi\cos\beta - \sin\gamma\sin\phi_f)(1-\cos\gamma) + \sin\phi\sin\beta\sin\gamma]$$

with r = OM, $\cos\beta = \sin\gamma\cos(\phi - \phi_f)$ where $\phi = (\vec{i}_o, -\vec{n})$ and $\phi_f = (\vec{i}_o, \vec{f})$. $\vec{f}$ is the unit vector projection of $\vec{F}$ on Π and $\vec{F}$ is the unit vector directing the flame. The different angles are illustrated in figure 4.

EXPERIMENTAL METHODOLGY

The experiments of fire are carried out in the Fire tunnel of CEREN laboratory situated in south of France (Marseille). This device is composed of a wind generator module and a combustion test module (see Fig. 5). Wind of constant velocity is produced by axial fans of variable rotational velocity. The air flow is guided between two concrete cell walls which are 8 m long, 2.75 m high and are spaced of 2.4 m. These walls allow to considerably reduce the contribution of lateral air in the combustion area. The pipe has a 1 m^2 cross section area and the maximum wind velocity is 8 m/s at the outlet. The combustion module is equipped with 4 vats made with steel. Vats are 2 m long, 2 m width and have a depth of 0.2 m. The middle of the first one contained straw to allow the fire priming in the *Quercus Coccifera*. The second one and the half of the third vat

contained straw and *Quercus Coccifera*. The loads were fixed at 1.5 kg/m^2 for straw with a thickness of about 10 cm and 3 kg/m^2 for *Quercus Coccifera* with an average thickness of 90 cm. Figure 6 shows the distribution of the vegetation in vats and the experimental apparatus.

The whole of this experimental apparatus is composed by a visual video camera (30 images/second, 640×480 pixels) and a wireless thermal sensor (Chetehouna *et al.*, 2008).

The heat fluxes measured by this wireless thermal sensor are noisy due to the flame oscillations caused by the turbulent flow surrounding the flame. This frequency perturbation is filtered by means of a low frequency filter of Butterworth of order 2 where its transfer function is:

$$\left|H(f)\right|^2 = \frac{1}{1+\left(\frac{f}{f_c}\right)^4} \qquad (12)$$

with f and f_c are respectively the frequency and the cut-off frequency. We choose a cut-off frequency $f_c = k\, f_p$ where k is a constant and f_p is the characteristic frequency of fire spread defined as the ratio between the rate of spread and the length of propagation zone.

Several fire experiments have been realized in the fire tunnel in order to study the effect of the wind (6 experiments for a *Quercus Coccifera* load of 3 kg/m^2 and wind values of 0, 0.5, 1, 1.5, 3 and 5 m/s) and the *Quercus Coccifera* load (4 experiments without wind for load values of 3, 4, 5 and 6 kg/m^2). In this paper we will only study the wind effect on the fire spread behavior to compare two flame models. **Let us notice that in the calculation of the two flame models, the thermal effects of the walls of the fire**

tunnel, described in this section, are neglected because they are designed in cellular-concrete material which is considered as a thermal insulator.

TESTING OF MODEL I AND MODEL II

While the ideal test for a mathematical model of the radiant heat flux would be against of a repeatable flame front, these are difficult to conduct experiments outside the laboratory. So, it is a challenge to obtain data providing sufficient information to relate fire characteristics under real conditions. **Nevertheless, the predictions from the two models (I and II) are first compared under no-wind condition to two radiative transfer models obtained by Monte Carlo Method and, secondly, to a previous model (Sparrow and Cess, 1978) detailed in appendix. Thirdly, these two simplified radiative flame models are confronted to six experiments carried out in a fire tunnel equipped with vats contained straw and *Quercus Coccifera*. In order to assess how the results of the models are affected by parameter uncertainly, the last section is devoted to a sensitivity analysis.**

Comparison between the two models and the Monte Carlo Method (Collin *et al.*, 2007) under no-wind condition

In this combustion problem, the flame and the surrounding air constitute a participating media for radiative transfer point of view. There is a variety of methods for modeling the radiative transfer problem such as Discrete Ordinates Method, Finite Volume Method, Monte Carlo Method … Among them the Monte Carlo Method can be easily applied to high complexity configurations due to the problem geometry for example.

The Monte Carlo Method is based on the following of several rays inside the medium in registering the successive paths and in modeling the emission, absorption and scattering

phenomena. The numerical results approach the exact solution of the radiative problem with a statistical error depending on the total number of the followed rays.

This technique has been already presented and used in various scientific fields (Collin *et al.*, 2007; Monod, 2009) and that is why this method is not detailed here. The main assumptions used in this work are that the surrounding air is supposed to be transparent, whereas the flame zone is participating to the radiative transfer. Indeed, a ray is followed from its emission inside the flame zone until the ray leaves the medium. In this work, two flame models are considered. The first flame model uses the radiant surface approach and the flame is characterized by its height, its width, its tilt angle, its temperature and the emissivity of the surface. In a second step, the flame is modeled by a volumetric source defined by its height, its width, its depth, its tilt angle, its temperature and the extinction coefficient representing the flame as an equivalent medium with homogeneous radiative properties. Figures 7.a and 7.b illustrate a theoretical comparison of results obtained by Monte Carlo Method using radiant surface approach (l_f = 1.6 m, $2L$ = 1 m, γ = 0, T_f = 1059 K and ε = 0.1) and volumetric source approach (l_f = 1.6 m, $2L$ = 1 m, d = 0.33 m, γ = 0, T_f = 1059 K and K_f = 0.1) with the results of model I and model II proposed here. It is shown that the results are in good agreement with those given by the two models and these models are considered valid regarding to a stochastic method.

Comparison between the two models and a previous model (Sparrow and Cess, 1978) under no-wind condition

Figure 8 presents predictions from the two flame models presented in this work and a model proposed by Sparrow and Cess (1978). We considered a vertical sensor located in front of a vertical flame front. We assumed a flame temperature of 1200 K, an atmospheric transmissivity of unity, a flame extinction coefficient of 0.2 m^{-1}, a flame

width of 20 m, a flame emissivity of 1 and a flame length of 3 m. The value of the flame depth (1.9 m) was then varied iteratively until that the predicted radiant heat flux (model II) matched as close as possible the predicted Sparrow and Cess radiant heat flux.

We can note that model I and II have practically the same accuracy than the flame model proposed by Sparrow and Cess (1978) for this theoretical case.

Comparison between experimental and numerical results

To test of the both models I and II, a comparison was done with results of six fire experiments in a fire large tunnel (2 m width) described above.

So, to calculate the heat flux, some parameters had to be determined. These parameters were the flame geometry variables (i.e. height, tilt angle, depth), equivalent flame emissivity, extinction coefficient into the flame, atmospheric transmissivity and flame temperature. The following assumption was made in the application of the model I: atmospheric transmissivity is equal to one (τ = 1). **Figure 9 illustrates a schematic view of the length, the height and the tilt angle of flame. These geometrical characteristics are obtained by means of a visual video camera (30 images/second, 640×480 pixels) showing the fire spread via a glass window placed in a lateral wall of the fire tunnel (see Figure 6). Their values are calculated for a thirty images and the mean values are given in the Table 1. The length of flame is considered as the distance between the highest pixel of flame and its base. The flame height is obtained by projection of the highest pixel of flame on the vertical axis. The tilt angle is calculated by the relation:**

$$\cos\gamma = \frac{h_f}{l_f} \qquad \textbf{(13)}$$

The extinction coefficient of the flame K_f is obtained by inverse method (Chetehouna *et al.*, 2008). This extinction coefficient value is 0.2 m^{-1}. We can note that is equal to the one given by Margerit and Séro-Guillaume (2002). In order to find the others parameters using the radiant heat measurements, we applied a *Mathematica Package: "GlobalOptimisation"* and the function *"NLRegression"*. This function performs nonlinear regression using nonlinear least-squares incorporating constraints which represent physical limits on the parameters being estimated. Values of these different parameters are given in Table 1.

The quality of the estimates from the both proposed models (I and II) was evaluated using a statistical performance measures. From the statistical measures, the normalized mean square error (NMSE), the fractional bias (FB) and the coefficient of determination (R^2) which are the most commonly used for model evaluation (Zàrate *et al.*, 2008; Muñoz *et al.*, 2004; Yadav and 1996) were chosen for the present analysis.

The NMSE is a measure of the degree of correlation. It provides information on the overall deviations between predicted and observed radiative heat flux. Its value should be as small as possible for a good model. NMSE is defined as:

$$NMSE = \frac{\overline{\left(\Phi^{\exp} - \Phi_{I,II}^{th}\right)^2}}{\overline{\Phi^{\exp}}.\overline{\Phi_{I,II}^{th}}} \qquad \textbf{(14)}$$

where overbars denote the mean values.

The FB indicates the degree of deviance. It provides information on the tendency of the model to overestimate or underestimate the measured values. The possible values of FB lie between – 2 and +2 and the desired value is zero. FB is given by:

$$FB = \frac{1}{0.5}\frac{\overline{\Phi^{\exp}} - \overline{\Phi^{th}_{I,II}}}{\overline{\Phi^{\exp}} + \overline{\Phi^{th}_{I,II}}} \qquad \textbf{(15)}$$

The R^2 describes the degree of agreement between the models. Its value lies between 0 and 1. For good performance of a model it should be close to unity. R^2 is defined as:

$$R^2 = \left(\frac{\frac{1}{n}\sum_{i=1}^{n}(\Phi^{\exp} - \overline{\Phi^{\exp}})(\Phi^{th}_{I,II} - \overline{\Phi^{th}_{I,II}})}{\sqrt{\frac{1}{n}\sum_{i=1}^{n}(\Phi^{\exp} - \overline{\Phi^{\exp}})^2}\sqrt{\frac{1}{n}\sum_{i=1}^{n}(\Phi^{th}_{I,II} - \overline{\Phi^{th}_{I,II}})^2}} \right)^2 \qquad \textbf{(16)}$$

where n is the number of observed values.

The statistical measures were computed for the entire data set (U = 0, 0.5, 1, 1.5, 3 and 5 m/s). The values of NMSE, FB and R^2 can be seen in Table 2. First of all, it can be observed, that the both models have a fairly good correlation and a small deviation. Secondly, it can be noted that the models I and II have practically the same accuracy. However, these approaches overestimate the experimental values and especially when the distance between the flame and the target increases (see Fig. 12). The variation of predicted values by the models must be attributed to the fact that the experimental data were obtained in outdoor fires under wind conditions. So, the determination of their geometry is a tricky challenge and contains a certain degree of subjectivity. New relevant methods are recently developed to determine fire front characteristics using vision technology (Rossi *et al.*, 2009; Akhloufi *et al.*, 2008) and must be used to improve prediction of radiant heat flux. Moreover, the proposed models consider an average temperature of flame for its entire area. But, the upper part of the flame has a less temperature

than the lower part (Muñoz *et al.*, 2004). So, when the distance between the flame and the target increases, the contribution of this area is overestimate. Though, despite the complicated nature of this study, these approaches produce fairly good predictions for the heat flux considering a thin flame approximation. The agreement between the models and the experimental values lends credibility to these models presented herein.

Sensitivity analysis

A simple univariate sensitivity analysis (Millington *et al.*, 2009) is used to assess how the results of the both models (I and II) are affected by parameter uncertainly. These parameters are: the tilt angle (γ), the height of the flame (h_f), the depth of the flame (d_f), the equivalent flame emissivity (ε), the flame temperature (T_f) and the extinction coefficient into the flame (K_f). Each input parameter is varied by ± 10 % of its default value, while all other parameters are held at their default value. Fig. 14 shows only the results for increases of parameters values (+ 10 %) but the conclusions are the same for decreases of them (-10 %). This analysis suggests that (i) the most sensitive parameter is the flame temperature for model I, (ii) that parameters with statistically effects on results are the flame temperature, the depth of flame and the extinction coefficient into the flame for model II, and (iii) that the tilt angle (γ), the height of the flame (h_f), and the equivalent flame emissivity (ε) have limited effects on the results of the models (I or II). So, this fact indicates that future use and refinement of these simplified flame models will examine new relevant methods to determine more precisely these parameters.

IMPLICATION FOR MODELING THERMAL RADIATION OF WIDLAND FIRES

The need to determine the heat flux from a wildland fire has lead to the development of numerous models. Based on the two models described above, we try in this section to determine the extent to which the range of assumptions made disqualifies some flame models from use.

Comparison between a blackbody box model and the two proposed models

The common assumption approximates the flame as a flat vertical sheet of given height and width with uniform temperature and emissivity. For large wildland fires, Butler and Cohen (1998) suggested a flame temperature of 1200 K and an emissivity of 1 (i.e. blackbody box model). However, this assumption means that predictions of heat flux may be inadequate. To illustrate this, we compared heat flux predicted by ours models against those calculated using this assumption under real conditions (U = 0.5 m/s). The values of the model parameters are given in Table 1. Figure 15 depicts that blackbody box model over-predicted the measured values. However, model I and model II accurately predicts the measured heat fluxes. This results show the necessity to calculate an equivalent emissivity for models using the assumption of a flame plane face emitting as a surface at a constant uniform temperature. Indeed, the assumption of an emissivity of unity negates the importance of the flame thickness in the heat flux modeling of this flame for outdoor fires.

Thermal radiation as a function of distance for different flame widths

The aim of some research teams is to create a simulator which is capable of describing the spread of a forest fire in order to help fire fighters facing a fire to make the appropriate decisions. This necessitates simple models capable of predicting the main

features of a fire with a low computational time. This aim has lead to the development and implementation of a number of radiant heat flux models. Because of the complex nature of wildland flames, a lot of assumptions are made. One of these assumptions is to consider that the fire front can be viewed as a flame panel of the same height and of infinite width from a surface target element. In order to investigate this approximation, the radiant heat flux was calculated for a given flame height (h_f = 1.6 m) and a given tilt angle (γ = 0) for three configurations: width equal to **2 m**, width equal to **4 m** and infinity width. Figure 16 shows that this approximation over-predicted the radiant heat flux and does not perform extremely well for positions near the fire front. So, in a future work, radiant heat flux models used to describe the spread of a wildland fire will be able to take into account the actual width of this fire front. Otherwise, the performance of the fire spread model may be compromised by inaccurate estimates of heat flux.

Thermal radiation as a function of distance for a same flame height

The basic physical model generally used to evaluate the heat flux is constructed around a representation of the flame front by a vertical opaque box located at the base of the flame front (Sullivan *et al*., 2003). By making the box vertical, the effect of the inclination of the flames is ignored. To illustrate this, we compared four modelled heat flux values for a same flame height (3 m) but with different flame length and flame inclination. Figure 17 depicts that the radiant heat flux is strongly dependent on tilt angle and flame length near the fire front. We can note that estimation of flame angle and flame length is critical to accurately predicting heat flux.

CONCLUSION

The aim of this paper is to compare and validate two flame models (I and II) for large fires under uniform wind condition, in a homogeneous and plane fuel bed. Experiments conducted in a Fire tunnel showed that the two flame models provide adequate results.

Model II considers a thin flame approximation and the equivalent emissivity value of 0.2 found with the analytical model I match the fact that the thicker the flames, the higher the emissivity of the flames (Sullivan *et al.*, 2003). We can note that no assumption about the flame emissivity is required for Model II derived from the Radiative Transfer Equation.

The need to calculate the heat flux from a large scale fire has lead to make a number of assumptions. So, in this work, the extent to which the range of assumptions made disqualifies a model from use is determined.

A validation of these two models with experimental data from real fires spreading would be quite desirable but it is difficult to obtain data of acceptable quality for wildland flame front geometry. It can be noted that for more accurate and realistic modeling of fire dynamics the turbulence/radiation interaction would have to be considered and present a challenge in the overall prediction of the heat flux emitted by a flame front in a wildland fire.

ACKNOWLEDGEMENT

The present work was partially supported by the Research National Agency under contract N° NT05-2_44411.

NOMENCLATURE

a	Absorption coefficient (m^{-1})
A_f	Surface of the flame on top of the fuel (m^2)
B	Stefan-Boltzmann constant ($W/m^2/K^4$)
$\boldsymbol{d_f}$	**Flame depth (m)**
d_o	Distance PM (m)
f	Frequency (Hz)
f_c	Cut-off frequency (Hz)
f_p	Characteristic frequency of fire spread (Hz)
$\vec{F}$	Unit vector directing the flame
$\vec{f}$	Unit vector projection of $\vec{F}$ on Π
$F_{i\to j}$	Dimensionless view factor between surface *i* and surface *j*
g	Acceleration due to gravity (m/s^2)
h_f	Flame height (m)
$\lvert H(f)\rvert^2$	Transfer function
I	Radiative intensity ($W/sr/m^2$)
I_b	Radiative intensity of blackbody ($W/sr/m^2$)
$\vec{i}_o$	Unit vector on the straight line (*Ox)*
$\vec{i}_n$	Unit vector on the straight line (*QM)*
K	Extinction coefficient (m^{-1})
K_f	Extinction coefficient into the flame (m^{-1})
K_v	Extinction coefficient into the vegetation (m^{-1})
L	Half width of the flame body (m)
l_f	Flame length (m)

$\vec{n}$	Unit vector, normal of the sensor
$\vec{N}$	Unit vector, normal of the fire front
r	Distance between the base of the fire front and the sensor (m)
R	Distance for view factor (m)
$\boldsymbol{R^2}$	**Coefficient of determination**
S	Flame surface (m^2)
T_f	Flame temperature (K)
x, y, z	Coordinate in space (m)
x_o, y_o, z_o	Coordinate in space (m)

Greek

β	Angle ($\vec{F}, \vec{w}_o$)
ε	Dimensionless equivalent flame emissivity
γ	Flame tilt angle
θ_f	Angle between ($0_0 M$)and (MF)
θ_f^a	Angle θ_f beneath the flame
θ_f^b	Angle θ_f ahead of the flame
θ_{fl}	Angle between R and the normal of fire front
θ_M	Angle between R and the normal of the target
σ_s	Scattering coefficient (m^{-1})
τ	Dimensionless atmospheric transmissivity
Ω_f	Flame domain
ω_i	Solid angle (sr)
ϕ	Angle $(\vec{i}_o, \vec{w}_o)$

ϕ_f	Angle $(\vec{i}_o, \vec{f})$
$\Phi^{\exp}$	**Experimental radiant heat flux (W/m^2)**
Φ_I^{th}	Radiant heat flux determinate using model I (W/m^2)
Φ_{II}^{th}	Radiant heat flux determinate using model II (W/m^2)
$\tilde{\Phi}$	Phase function
ψ	Angle between (*OM)* and (*PM)*

APPENDIX

Sparrow and Cess view factor

The view factor between a vertical sensor (M) and a vertical flame front can be written (Sparrow and Cess, 1978):

$$F_{f\to M}(\mathbf{M}) = \frac{1}{2\pi}\left[\frac{X}{\sqrt{1+X^2}}\arctan\left(\frac{Y}{\sqrt{1+X^2}}\right)+\frac{Y}{\sqrt{1+Y^2}}\arctan\left(\frac{X}{\sqrt{1+Y^2}}\right)\right]$$

with $X = \frac{a}{c}$ and $Y = \frac{b}{c}$ (see Fig. A1).

Heat flux using Sparrow and Cess view factor

$$\boldsymbol{\Phi(\mathbf{M}) = \tau\,\varepsilon\,B\,T_f^4\;F_{f\to M}}$$

Heat flux using the infinity width assumption

$$\Phi(\mathbf{M}) = \frac{\tau\,\varepsilon\,B}{2}\,T_f^4\;(1-\cos\theta_f)$$

REFERENCES

Akhloufi M., Rossi L., Abdelhadi L and Tison Y. (2008) Image Processing theory, tools and applications, research – development- application, pp. 68 – 74, Ed. Dorra Sallemi Masmoudi, Khalifa Djamel.

Balbi J.H., Rossi J.L., Marcelli T. and Santoni P.A. (2007) A 3D physical real-time model of surface fires across fuel beds. *Combustion Science and Technology*, 179 (12), 2511-2537.

Baukal C.E., Gebhart B. (1997) Oxygen-enhanced/natural gas flame radiation. *International Journal of Heat and Mass Transfer*, 40 (11), 2539-2547.

Butler B.W. and Cohen J.D. (1998) Firefighter Safety Zones: A Theoretical Model Based on Radiative Heating. *International Journal of Wildland Fire*, 8 (2), 73-77.

Chetehouna K., Séro-Guillaume O., Degiovanni, A. (2005) Identification of the upward gas flow velocity and of the geometric characteristics of a flame with a specific thermal sensor. *International Journal of Thermal Sciences*, 44 (10), 966-972.

Chetehouna K., Séro-Guillaume O., Sochet I., Degiovanni A. (2008) On the experimental determination of flame front positions and of propagation parameters for a fire. *International Journal of Thermal Sciences*, 47 (9), 1148-1157.

Collin A., Boulet P., Parent G., Lacroix D. (2007) Numerical simulation of a water spray - Radiation attenuation related to spray dynamics. *International Journal of Thermal Sciences*, 46(9), 856-868.

Monod B., Collin A., Parent G., Boulet P. (2009) Infrared radiative properties of vegetation involved in forest fires. *Fire Safety Journal*, 44 (1), 88-95.

Dupuy, J.L. (2000) Testing Two Radiative Physical Models for Fire Spread Through Porous Forest Fuel Beds. *Combustion Science and Technology*, 155(1), 149-180.

Knight I.K. and Sullivan A.L. (2004) A semi-transparent model of bushfires flames to predict radiant heat flux. *International Journal of Wildland Fire*, 13, 201-207.

Margerit J. and Séro-Guillaume O. (2002) Modelling forest fires. Part II: reduction to two-dimensional models and simulation of propagation. *International Journal of Thermal Sciences*, 45 (8), 1723-1737.

Millington J.D.A., Wainwright J., Perry G.L.W., Romero-Calcerrada R., Malamud B.D. (2009). Modelling Mediterranean landscape succession-disturbance dynamics: A landscape fire-succession model. *Environmental Modelling & Software*, 24, 1196-1208.

Monod B., Collin A., Parent G. and Boulet P. (2009) Infrared radiative properties of vegetation involved in forest fires. *Fire Safety Journal*, 44(1), 88-95.

Morandini F., Santoni P.A. and Balbi J.H. (2001) The contribution of radiant heat transfer to laboratory-scale fire spread under the influences of wind and slope. *Fire Safety Journal*, 36, 519-543.

Morvan D., Méradji S. and Accary G. (2008) Physical modelling of fire spread in Grasslands. *Fire Safety Journal*, 44 (1), 50-61.

Muñoz M., Arnaldo J., Casal J. and Planas E. (2004). Analysis of the geometric and radiative characteristics of hydrocarbon pool fires. *Combustion and Flame*, 139, 263-277.

Raj P.K. (2008) A review of the criteria for people exposure to radiant heat flux from fires. *Journal of Hazardous Materials*, 159, 61-71.

Rossi L., Akhloufi M. and Tison Y. (2009). Dynamic fire 3D modeling using a real-time stereovision system. *Journal of Communication and Computer*, 6 (10), 541-61.

Sacadura J.F. (2005) Radiative heat transfer in fire safety science. *Journal of Quantitative Spectroscopy & Radiative Transfer*, 93 (1-3), 5-24.

Séro-Guillaume O., Ramezani S., Margerit J., Calogine D. (2008) On large scale forest fires propagation models. *International Journal of Thermal Sciences*, 47 (6), 680-694.

Siegel R., Howell J. (2002) Thermal radiation heat transfer – fourth ed., Taylor & Francis, New York.

Sparrow, E.M. and Cess, R.C. (1978) Radiation Heat Transfer – Augmented ed., Hemisphere, Washington, D.C.

Sullivan A.L., Ellis P.F. and Knight I.K. (2003) A review of radiant heat flux models used in bushfire applications. *International Journal of Wildland Fire*, 12, 101-110.

Viegas, D.X. (2004) On the existence of a steady state regime for slope and wind driven fires. *International Journal of Wildland Fire*, 13, 101-117.

Viskanta R. (2008) Overview of some radiative transfer issues in simulation of unwanted fires. *International Journal of Thermal Sciences*, 47, 1563-1570.

Yadav A. K. and Sharan M. (1996). Statistical evaluation of sigma scheme for estimating dispersion in low wind conditions. *Atmospheric Environment,* 30 (14), 2595-2606.

Zàrate L, Arnaldos J. and Casal J. (2008) Establishing safety distances for wildland fires. *Fire Safety Journal*, 43, 565-575.

List of figures

Figure. 14. Sensitivity analysis **(default values: T_f = 1059 K, ε = 0.2, γ = 0, h_f = 1.6 m, d_f = 0.33 m, K_f = 0.2 m^{-1})**.

Figure. 15. Comparison between a blackbody box model **(T_f = 1200 K and ε = 1) for a *Quercus Coccifera* load of 3 kg/m^2 and wind value of 0.5 m/s (T_f = 1134 K, K_f = 0.2 m^{-1} and ε = 0.2).**

Figure. 16. Thermal radiation flux as a function of the distance **for a *Quercus Coccifera* load of 3 kg/m^2 and wind value of 0 m/s and for several flame widths (h_f = 1.6 m, γ = 0, T_f = 1059 K, d_f = 0.33 m, K_f = 0.2 m^{-1} and ε = 0.2)**.

Figure. 17. Thermal radiation flux as a function of the distance for a flame height of 3 m **(T_f = 1200 K and ε = 1)**.

Figure. A1. Schematic of geometry used to calculate the view factor proposed by Sparrow and Cess (1978).

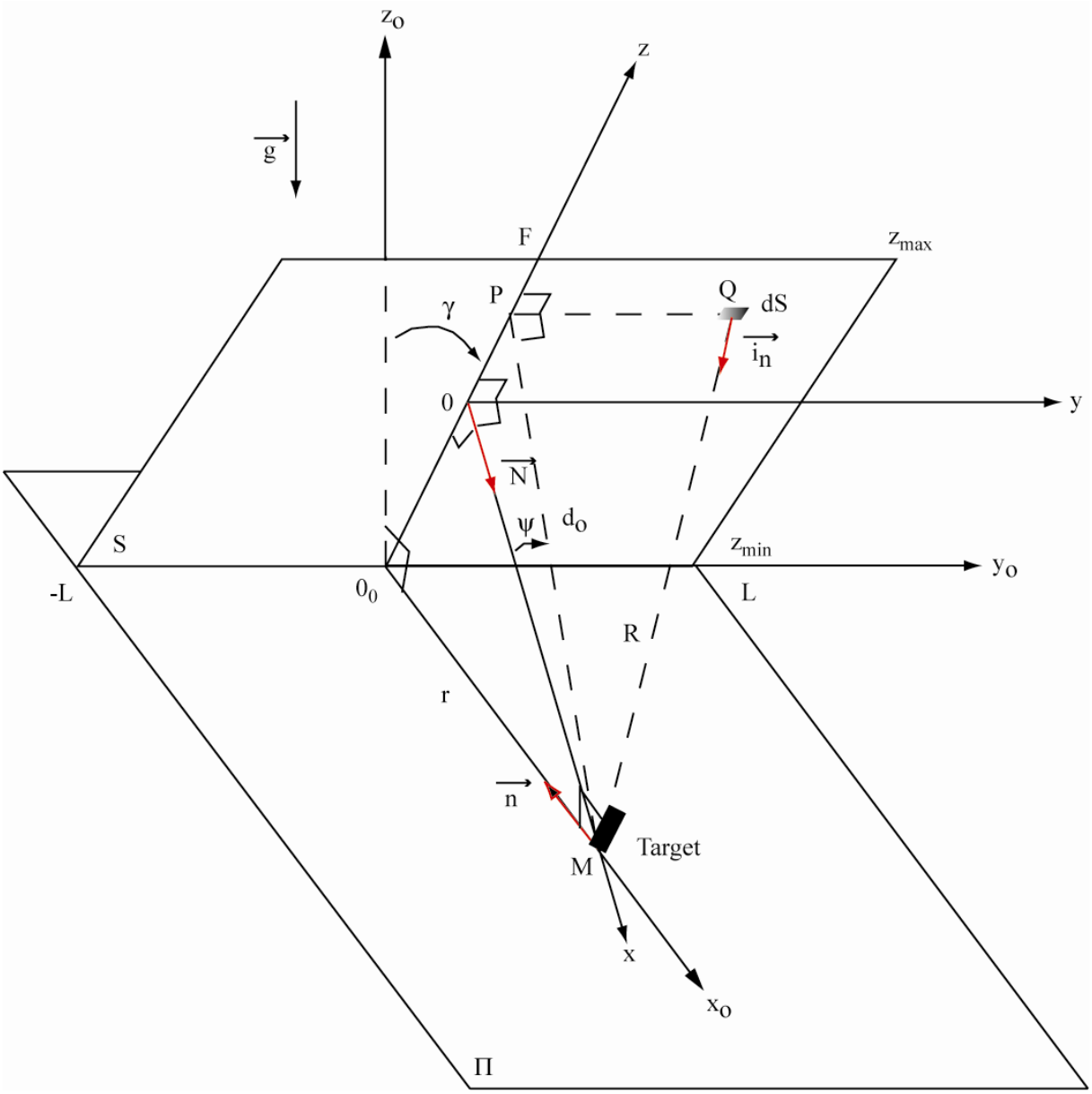

Figure 1.

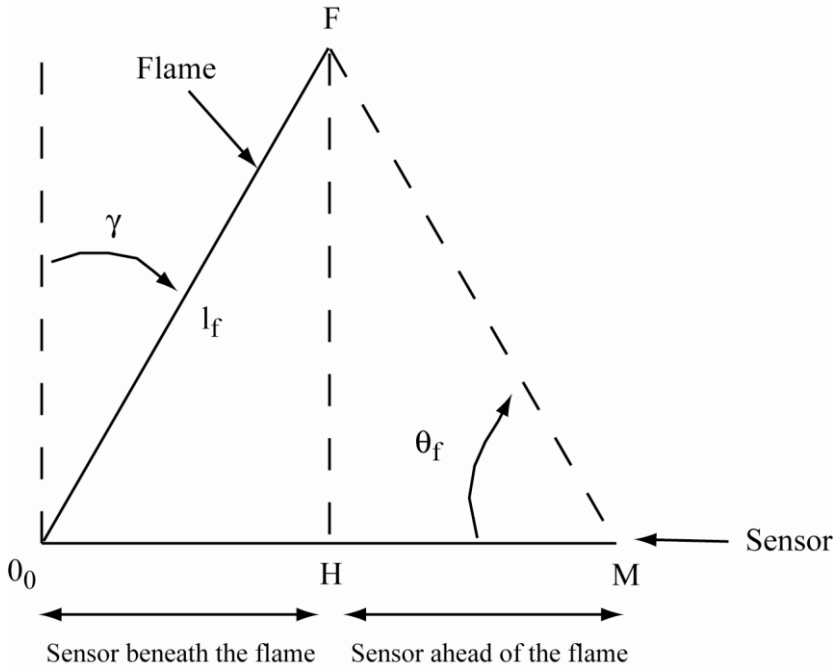
F
Flame
γ
l_f
θ_f
Sensor
0_0
H
M
Sensor beneath the flame
Sensor ahead of the flame

Figure 2.

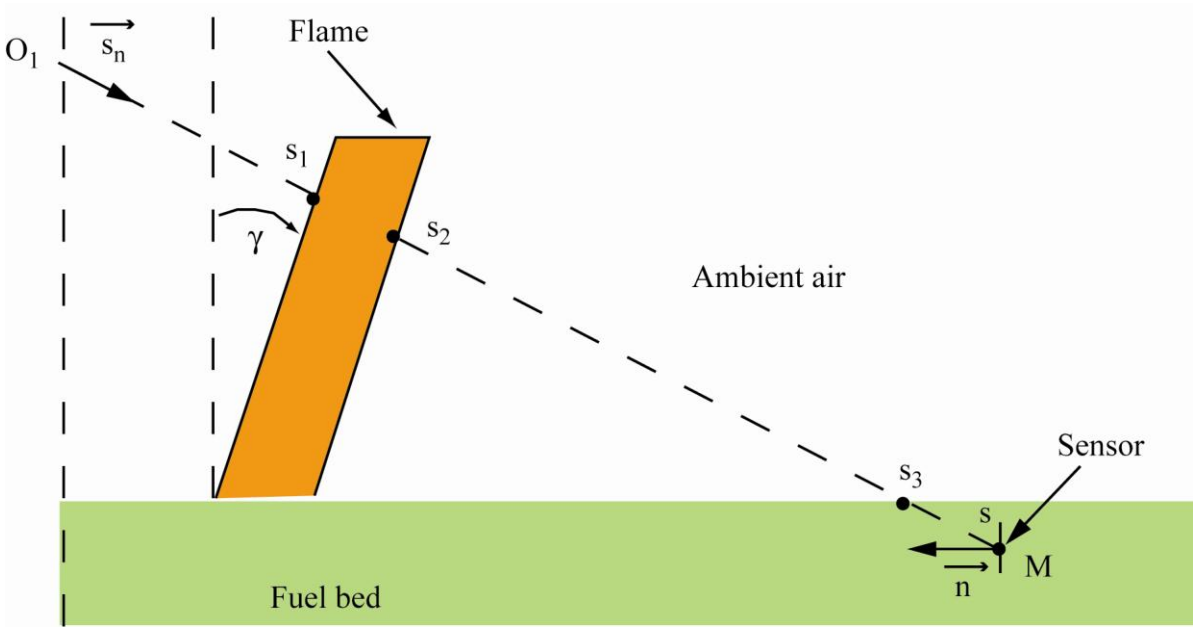

Figure 3.

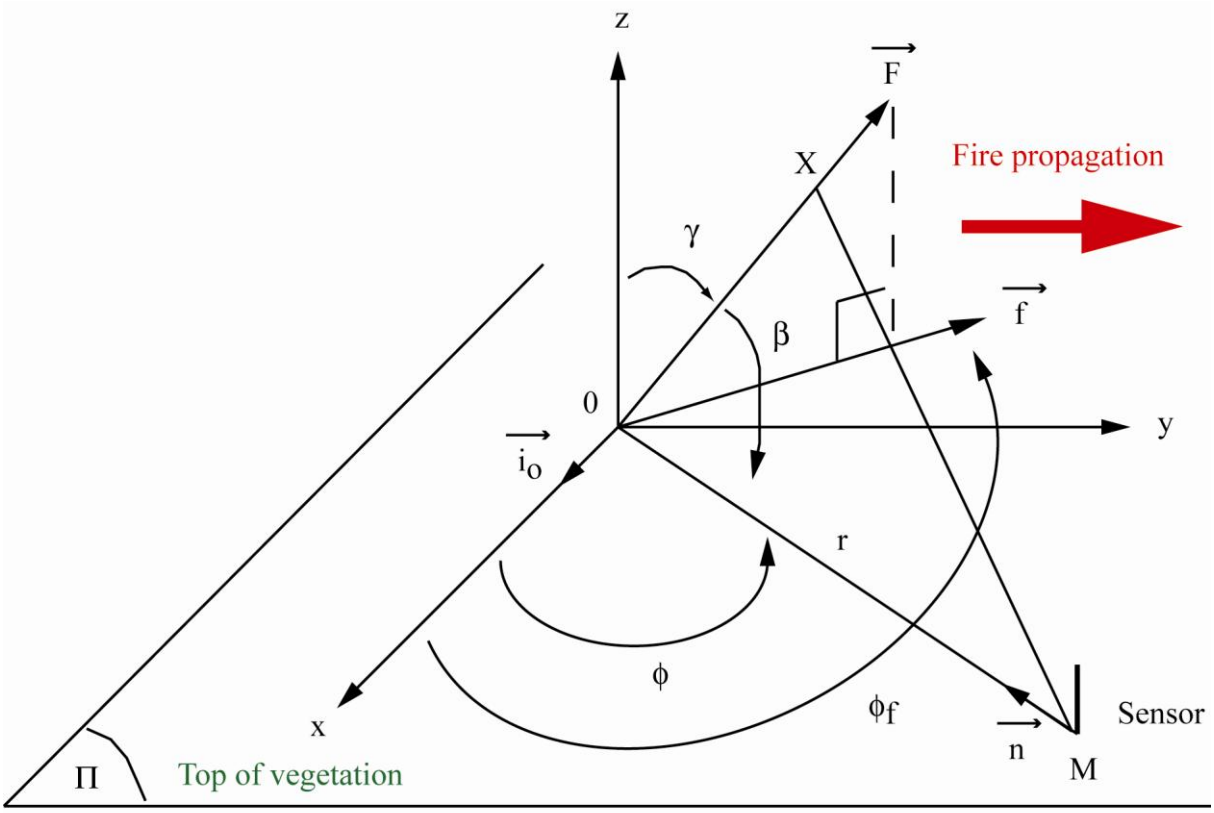
z
F
X
Fire propagation
γ
β
f
0
y
i_o
r
ϕ
ϕf
x
Sensor
n
M
Π
Top of vegetation

Figure 4.

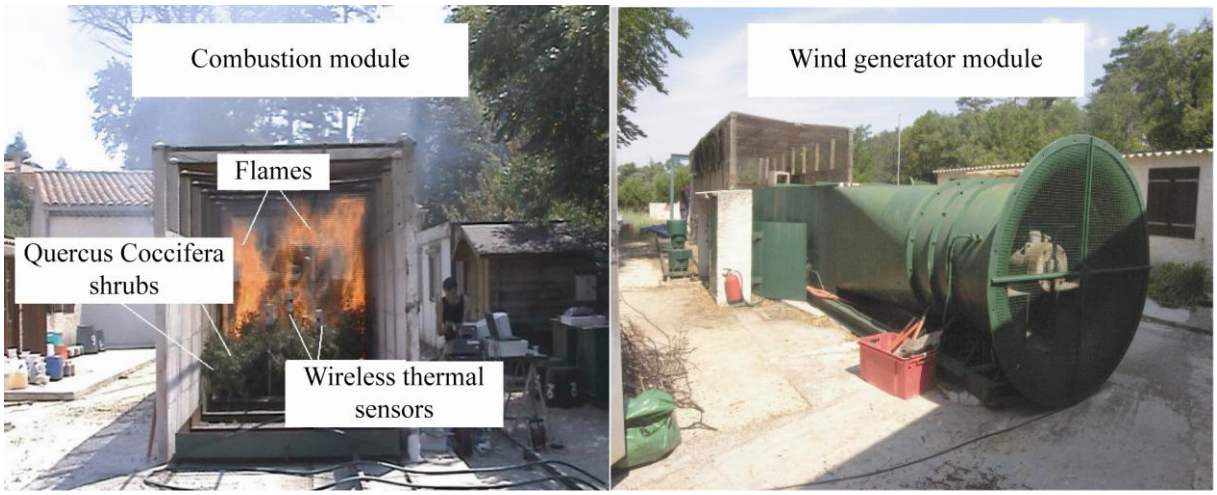
Combustion module
Flames
Quercus Coccifera shrubs
Wireless thermal sensors
Wind generator module

Figure 5.

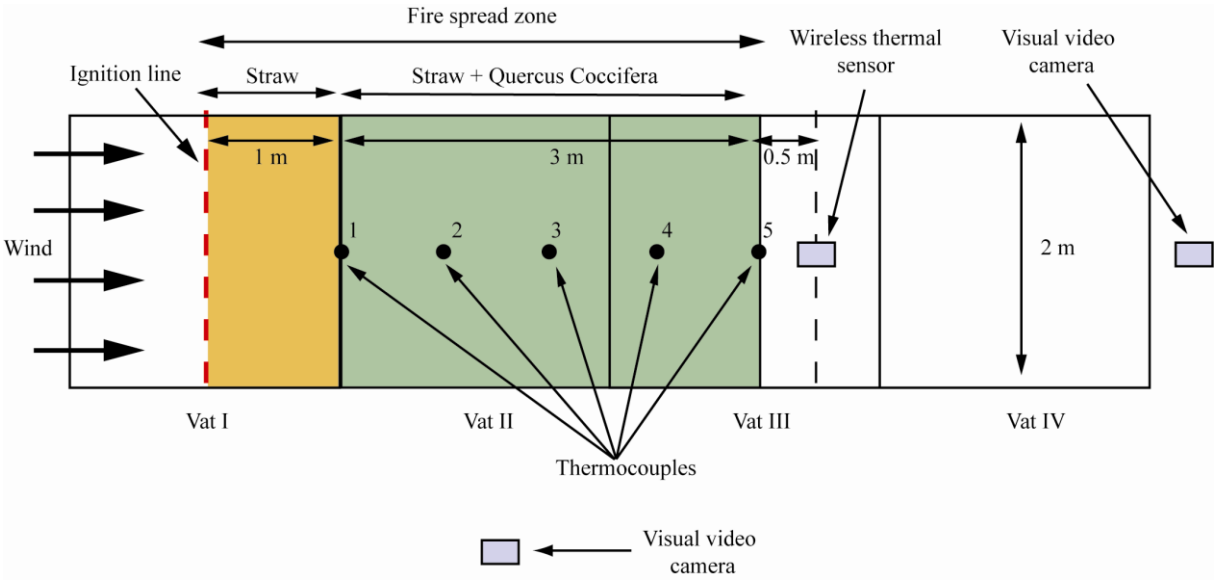
Fire spread zone
Wireless thermal sensor
Visual video camera
Ignition line
Straw
Straw + Quercus Coccifera
1 m
3 m
0.5 m
Wind
1
2
3
4
5
2 m
Vat I
Vat II
Vat III
Vat IV
Thermocouples
Visual video camera

Figure 6.

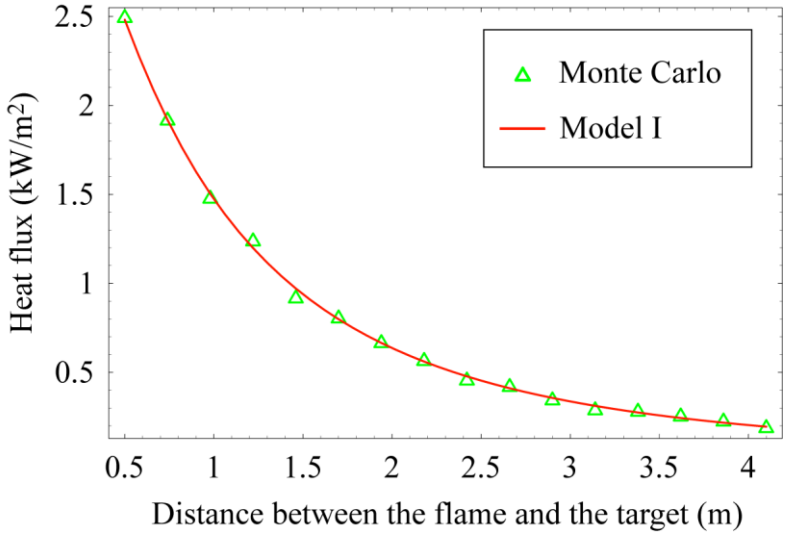
Heat flux (kW/m²)
2.5
2
1.5
1
0.5
0.5
1
1.5
2
2.5
3
3.5
4
Distance between the flame and the target (m)
Monte Carlo
Model I

Figure 7.a.

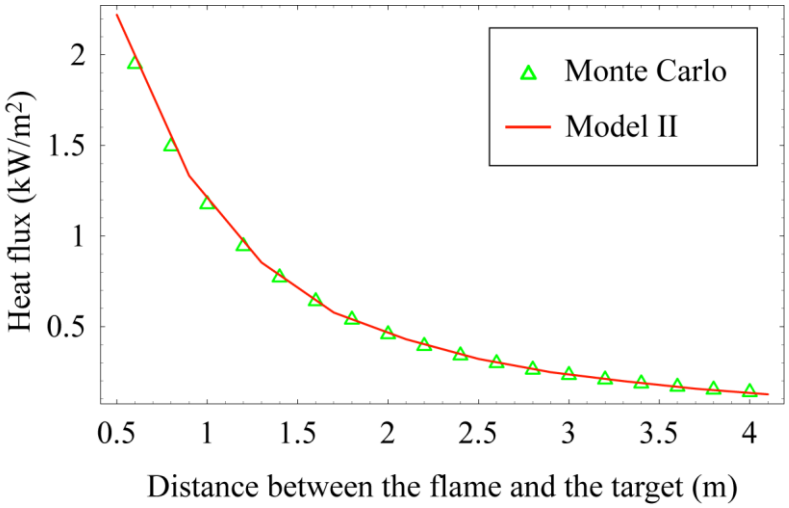
Monte Carlo
Model II
Heat flux (kW/m²)
2
1.5
1
0.5
0.5
1
1.5
2
2.5
3
3.5
4
Distance between the flame and the target (m)

Figure 7.b.

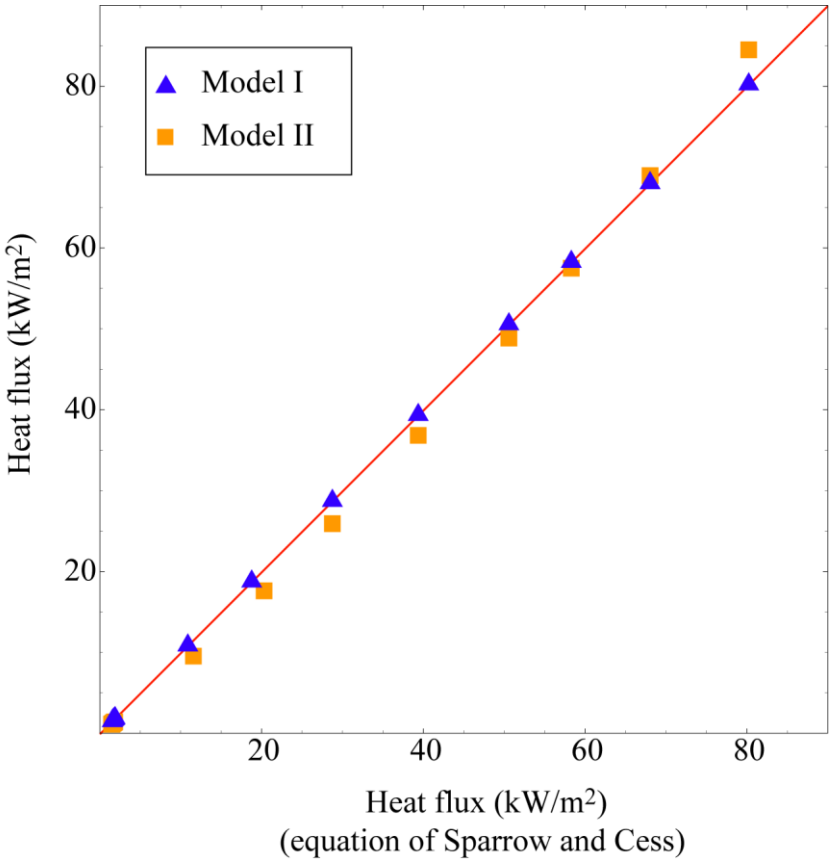
Model I
Model II
80
60
40
20
Heat flux (kW/m2)
20
40
60
80
Heat flux (kW/m2)
(equation of Sparrow and Cess)

Figure 8.

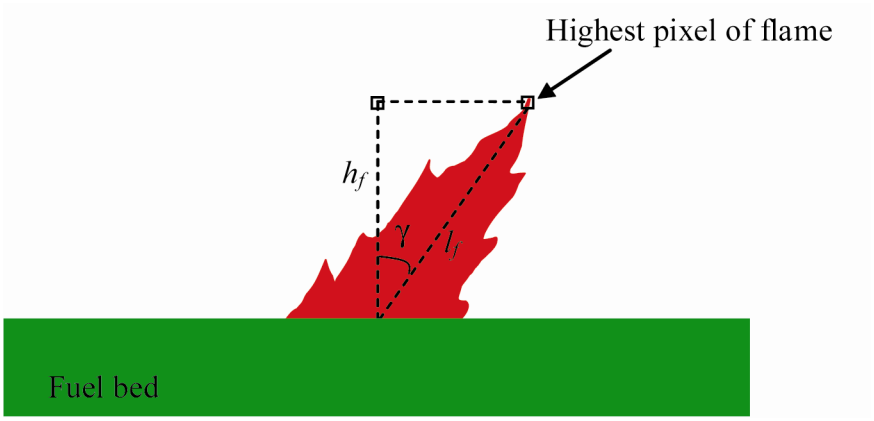

Figure 9.

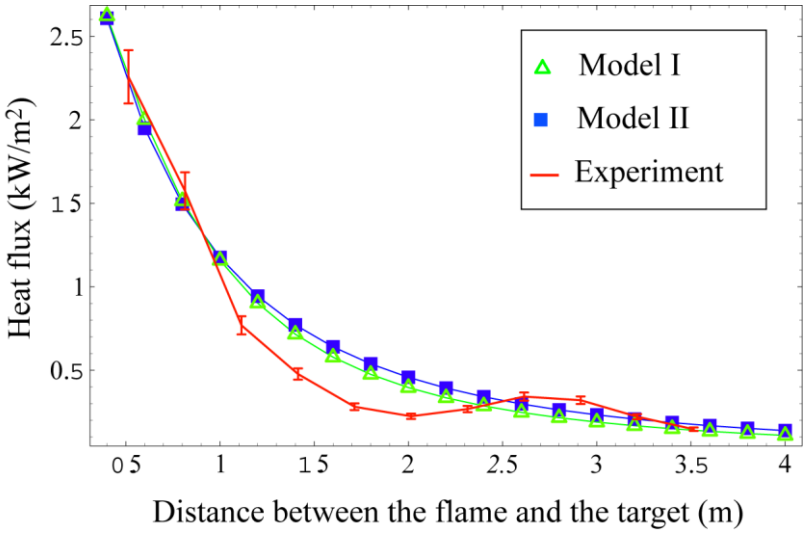
Heat flux (kW/m2)
2.5
2
1.5
1
0.5
0.5
1
1.5
2
2.5
3
3.5
4
Distance between the flame and the target (m)
Model I
Model II
Experiment

Figure 10.

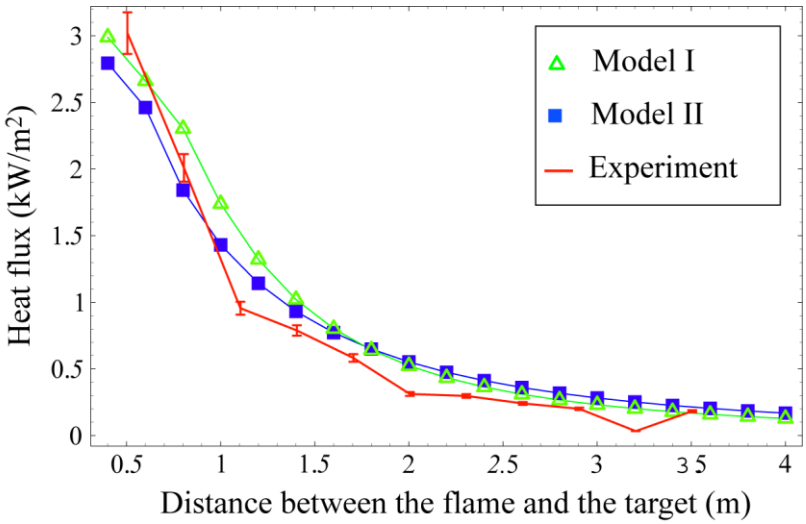
Model I
Model II
Experiment
Heat flux (kW/m2)
Distance between the flame and the target (m)
0
0.5
1
1.5
2
2.5
3
0.5
1
1.5
2
2.5
3
3 5
4

Figure 11.

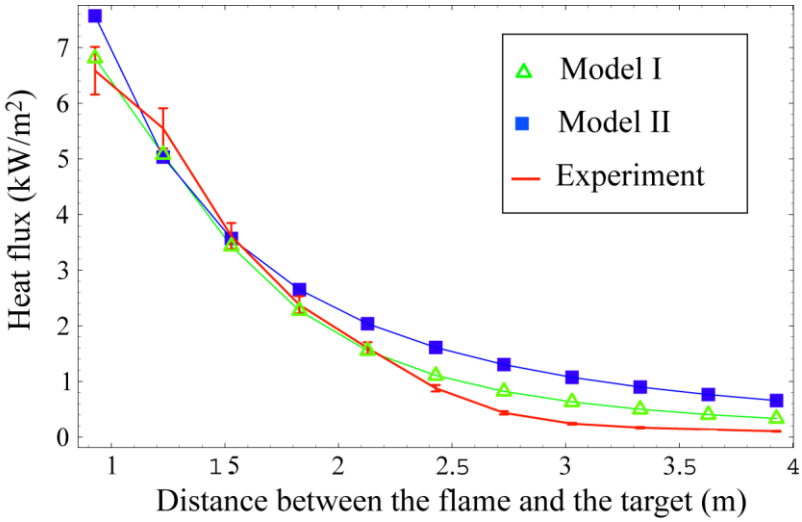
Heat flux (kW/m2)
Distance between the flame and the target (m)
Model I
Model II
Experiment
0
1
2
3
4
5
6
7
1
1.5
2
2.5
3
3.5
4

Figure 12.

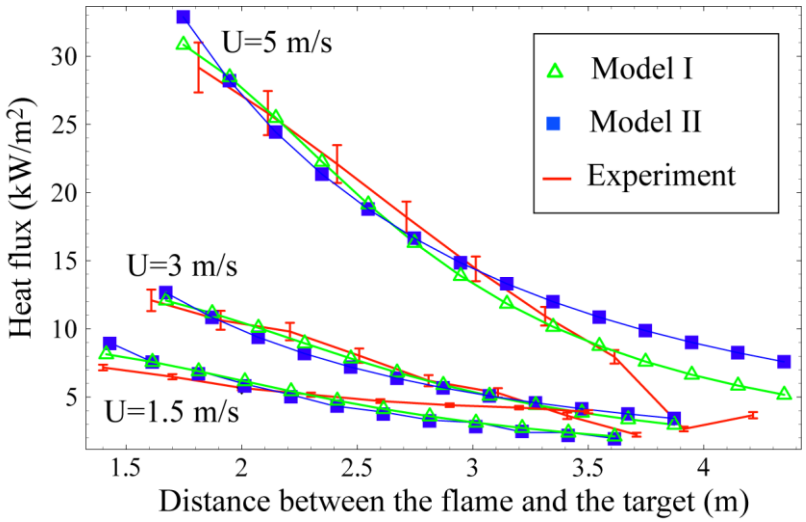
U=5 m/s
U=3 m/s
U=1.5 m/s
Model I
Model II
Experiment
Heat flux (kW/m²)
Distance between the flame and the target (m)
30
25
20
15
10
5
1.5
2
2.5
3
3.5
4

Figure 13.

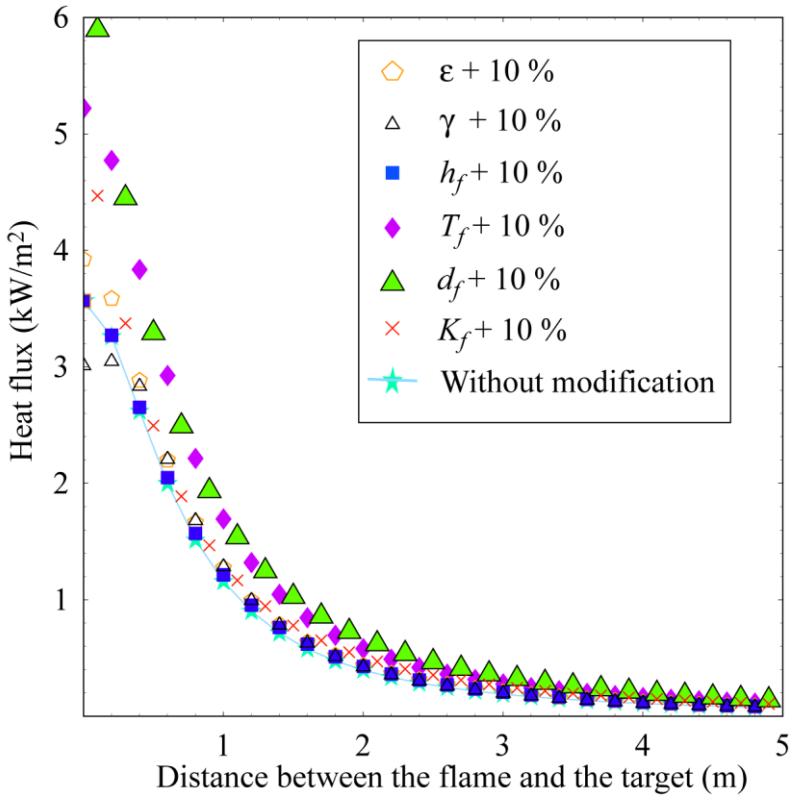
Heat flux (kW/m²)
Distance between the flame and the target (m)
ε + 10 %
γ + 10 %
h_f + 10 %
T_f + 10 %
d_f + 10 %
K_f + 10 %
Without modification
1
2
3
4
5
6

Figure 14.

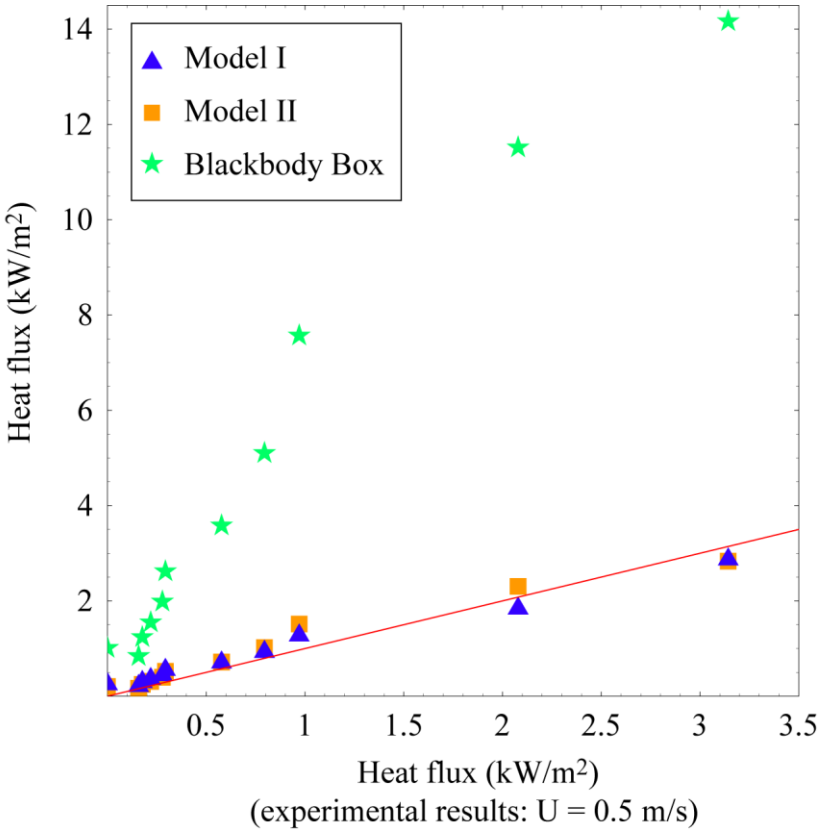
Model I
Model II
Blackbody Box
Heat flux (kW/m2)
14
12
10
8
6
4
2
0.5
1
1.5
2
2.5
3
3.5
Heat flux (kW/m2)
(experimental results: U = 0.5 m/s)

Figure 15

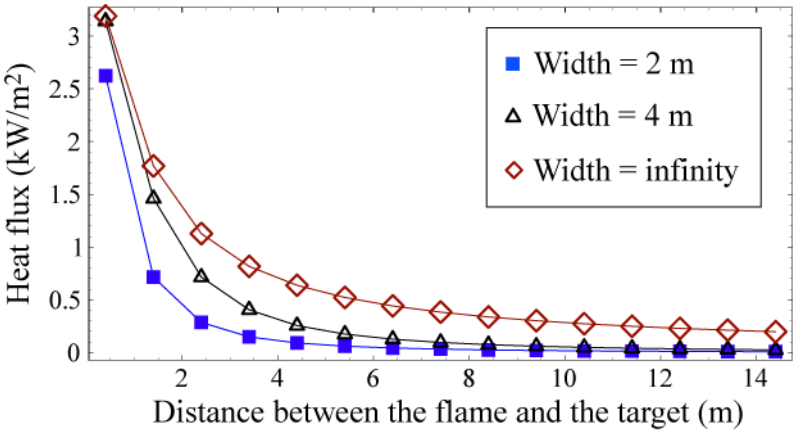
Heat flux (kW/m²)
Distance between the flame and the target (m)
Width = 2 m
Width = 4 m
Width = infinity
0
0.5
1
1.5
2
2.5
3
2
4
6
8
10
12
14

Figure 16.

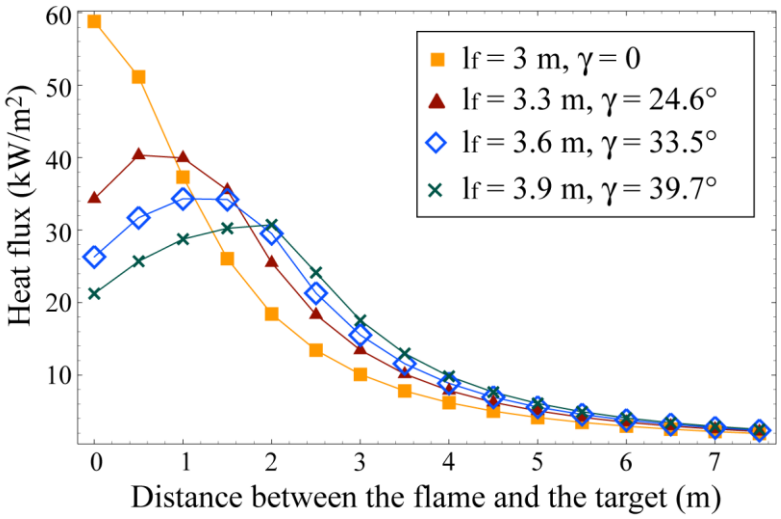
Heat flux (kW/m²)
60
50
40
30
20
10
0
1
2
3
4
5
6
7
Distance between the flame and the target (m)
lf = 3 m, γ = 0
lf = 3.3 m, γ = 24.6°
lf = 3.6 m, γ = 33.5°
lf = 3.9 m, γ = 39.7°

Figure 17.

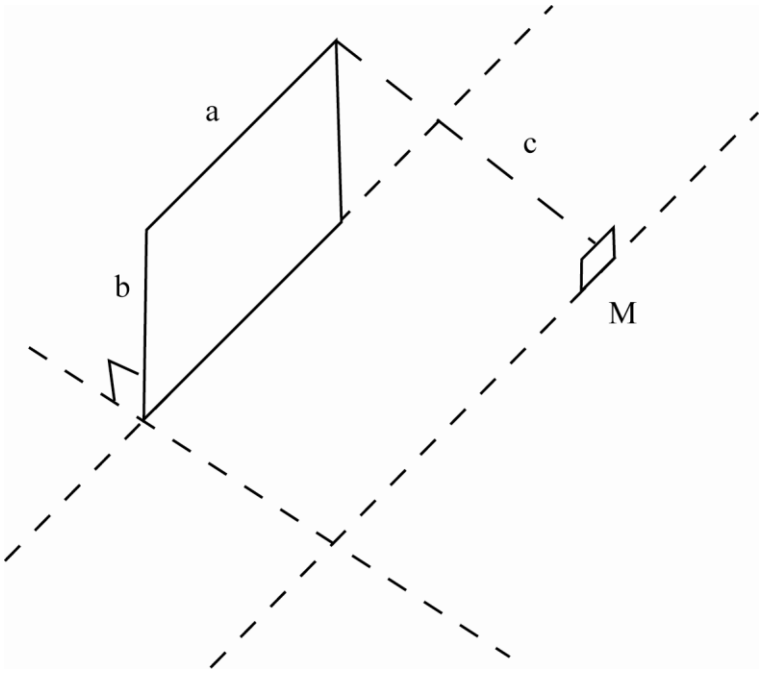

Figure A1.

List of tables

Wind (m/s)	Height (m)	Tilt angle (°)	Depth (m)	Temperature (°K)	Emissivity
0	1.6	0	0.33	1059	0.2
0.5	1.55	24.1	0.33	1134	0.2
1	1.42	41.3	0.33	1092	0.2
1.5	1.31	47.2	0.38	1160	0.2
3	1.29	52.1	0.44	1333	0.2
5	1.14	57.1	0.5	1675	0.2

Table 1.

	NMSE	FB	R^2
Model I	0.035	- 0.085	0.99
Model II	0.1	- 0.173	0.98

Table 2.